Available online at www.sciencedirect.com
SCIENCE DIRECT®
International Journal of Solids and Structures 43 (2006) 459–474
INTERNATIONAL JOURNAL OF SOLIDS and STRUCTURES
www.elsevier.com/locate/ijsolstr

Effect of notch depth on strain-concentration factor of rectangular bars with a single-edge notch under pure bending

H.M. Tlilan *, N. Sakai, T. Majima

Department of Electronics and Mechanical Sciences, Graduate School of Science and Technology, Chiba University, 1-33, Yayoicho, Inage-ku, Chiba 263-8522, Japan

Received 13 September 2004; received in revised form 24 March 2005
Available online 26 May 2005

Abstract

The FEM is employed to study the effect of notch depth on a new strain-concentration factor (SNCF) for rectangular bars with a single-edge notch under pure bending. The new SNCF $K_{\varepsilon}^{\mathrm{new}}$ is defined under the triaxial stress state at the net section. The elastic SNCF increases as the net-to-gross thickness ratio h_0/H_0 increases and reaches a maximum at $h_0/H_0 = 0.8$. Beyond this value of h_0/H_0 it rapidly decreases to the unity with h_0/H_0. Three notch depths were selected to discuss the effect of notch depth on the elastic–plastic SNCF; they are the extremely deep notch ($h_0/H_0 = 0.20$), the deep notch ($h_0/H_0 = 0.60$) and the shallow notch ($h_0/H_0 = 0.95$). The new SNCF increases from its elastic value to the maximum as plastic deformation develops from the notch root. The maximum $K_{\varepsilon}^{\mathrm{new}}$ of the shallow notch is considerably greater than that of the deep notch. The elastic $K_{\varepsilon}^{\mathrm{new}}$ of the shallow notch is however less than that of the deep notch. Plastic deformation therefore has a strong effect on the increase in $K_{\varepsilon}^{\mathrm{new}}$ of the shallow notch. The variation in $K_{\varepsilon}^{\mathrm{new}}$ with M/M_{Y}, the ratio of bending moment to that at yielding at the notch root, is slightly dependent up to the maximum $K_{\varepsilon}^{\mathrm{new}}$ for the shallow notch. This dependence is remarkable beyond the maximum $K_{\varepsilon}^{\mathrm{new}}$. On the other hand, the variation in $K_{\varepsilon}^{\mathrm{new}}$ with M/M_{Y} is independent of the stress–strain curve for the deep and extremely deep notches.

Keywords: Pure bending; Shallow notch; Single-edge notch; Strain-concentration factor; Finite element method

Abbreviations: GY, general yielding; SNCF, strain-concentration factor; SSCF, stress-concentration factor.

* Corresponding author. Tel./fax: +81 432461820.
E-mail address: tlilan@graduate.chiba-u.jp (H.M. Tlilan).

0020-7683/$ - see front matter © 2005 Elsevier Ltd. All rights reserved.
doi:10.1016/j.ijsolstr.2005.03.069

Nomenclature

a_0, a	initial and current distances, respectively, from the transverse load to support (see Fig. 2)
b_0	width of notched rectangular bar
E	Young's modulus
h_c	current height under compressive ε_x at the net section (see Fig. 1)
h_t	current height under tensile ε_x at the net section (see Fig. 1)
h_0	initial thickness at the net section (see Fig. 1)
H_0	initial thickness at the gross section (see Fig. 1)
K_ε^{con}	conventional SNCF
K_ε^{new}	new SNCF
M	bending moment per unit width $= Pa$ (N mm/mm)
M_Y	M at yielding at the notch root (N mm/mm)
P	transverse load per unit width (N/mm) (see Fig. 2)
ε_n^{con}	conventional nominal strain
ε_n^{new}	new nominal strain $= \varepsilon_n^t =$ Maximum tensile longitudinal strain obtained from the assumed linear distribution (see Fig. 1)
ε_x	longitudinal strain
$(\varepsilon_x^t)_{max}$	maximum tensile longitudinal strain at the notch root
ν	Poisson's ratio
ξ	distance from the current centre of the net section (see Fig. 1)
ρ_0	initial notch radius (see Fig. 1)
σ_{eq}	equivalent stress $= \{(\sigma_x-\sigma_y)^2+(\sigma_y-\sigma_z)^2+(\sigma_z-\sigma_x)^2\}^{1/2}/\sqrt{2}$
σ_x	longitudinal stress
σ_y	transverse stress
σ_z	stress in the width direction
σ_Y	tensile yield stress
ϕ	$= 6/E(h_t+h_c)^2$
ψ	distance from the current neutral surface (see Fig. 1)

1. Introduction

Many analytical, numerical and experimental studies have been done on the elastic stress-concentration factor (SSCF) for various types of notch under tension and under bending (Leven and Frocht, 1952; Nishida, 1974; Kato, 1991; Noda et al., 1995; Pilkey, 1997). Neuber's analytical results have been the main source for the effect of notch depth on the elastic SSCF Pilkey (1997). The results indicate that the elastic SSCF rapidly decreases with decreasing notch depth from the maximum value at an intermediate notch depth. This indicates that the elastic SSCF of a shallow notch is much less than that of a notch with an intermediate notch depth. However, little attention has been paid to the elastic strain- concentration factor (SNCF).

The effect of plastic deformation in the vicinity of the notch root on the SSCF and the SNCF has been studied under axial tension. The studies on the elastic–plastic SSCF and SNCF have been reviewed in a previous paper Majima (1999). These studies indicate that the SSCF decreases from its elastic value towards unity. On the other hand, Majima (1999) has proposed a new SNCF for axial tension. This new SNCF increases from its elastic value as plastic deformation develops from the notch root and maintains a high value even after general yielding. These results indicate that the SNCF is more important than the SSCF.

The proposed new SNCF has been defined under the triaxial stress state at the net section (Majima, 1999). This has enabled the new SNCF to provide the reasonable values consistent with concave distributions of the axial strain on the net section. Moreover, the new SNCF has removed the contradiction resulting from the definition of the conventional SNCF. That is, the conventional SNCF provides the values less than unity in spite of the concave distributions of the axial strain under elastic–plastic deformation (Majima, 1999). The average axial strain, or the nominal strain, of the conventional SNCF has been defined under the uniaxial stress state (Neuber, 1961), completely unrelated to the stress state at the net section (Majima, 1999). This difference in the stress state causes the above contradiction in the conventional SNCF. This means that the SNCF for any type of loading should be defined under the triaxial stress state at the net section.

Few studies have been done on the elastic–plastic strain concentration under bending. It follows that the effect of notch depth has not been evaluated on the elastic–plastic SNCF under bending. A new definition of the elastic–plastic SNCF for bending has been proposed by Majima and Ishizaka (2003) and applied to plane-strain rectangular bars with symmetrical notches under pure bending. The nominal strain for this new SNCF has been defined under the triaxial stress state at the net section. This new SNCF has been successful to provide the reasonable values for the non-linear distribution of the longitudinal strain on the net section (Majima and Ishizaka, 2003).

The aim of this study is to examine the effect of notch depth on the elastic–plastic new SNCF of plane-strain rectangular bars with a single-edge notch under pure bending. The strain distributions on the net section were obtained using a finite element method (FEM). The FEM calculations were performed up to a deformation level slightly beyond general yielding. The materials employed are an Austenitic stainless steel and an Ni–Cr–Mo steel.

2. The definition of the new SNCF

The proposed new SNCF for pure bending has been defined as the ratio of the maximum tensile longitudinal strain at the notch root $(\varepsilon_x^{\mathrm{t}})_{\max}$ to the new nominal strain $\varepsilon_{\mathrm{n}}^{\mathrm{new}}$ (Majima and Ishizaka, 2003), i.e.

$$K_{\varepsilon}^{\mathrm{new}} = \frac{(\varepsilon_x^{\mathrm{t}})_{\max}}{\varepsilon_{\mathrm{n}}^{\mathrm{new}}} \tag{1}$$

Since $(\varepsilon_x^{\mathrm{t}})_{\max}$ is the actual longitudinal strain at the notch root, $(\varepsilon_x^{\mathrm{t}})_{\max}$ is independent of definition. The new SNCF is thus presented by defining a new nominal strain.

The longitudinal strain ε_x can be assumed to have a linear distribution on the net section if the notch effect is negligible. Fig. 1 schematically shows the non-linear distribution of ε_x and this assumed linear distribution. A new nominal strain is therefore given by the maximum tensile longitudinal strain obtained from this assumed linear distribution at the notch root, $\varepsilon_{\mathrm{n}}^{\mathrm{t}}$.

The assumed linear distribution is determined by the following equation (Majima and Ishizaka, 2003):

$$\int_{-h_{\mathrm{c}}}^{h_{\mathrm{t}}} \varepsilon_x b_0 \psi \,\mathrm{d}\psi = \int_{-(h_{\mathrm{t}}+h_{\mathrm{c}})/2}^{(h_{\mathrm{t}}+h_{\mathrm{c}})/2} \varepsilon_{\mathrm{n}}^{\mathrm{t}} \frac{2\xi}{(h_{\mathrm{t}}+h_{\mathrm{c}})} b_0 \xi \,\mathrm{d}\xi \tag{2}$$

where h_{t} and h_{c} are the current heights from the neutral surface to the notch root and to the unnotched surface opposite to the notch root, respectively. The values of h_{t} and h_{c} change with deformation, and hence the left-hand side of Eq. (2) should be integrated between the current limits $-h_{\mathrm{c}}$ and h_{t}. On the other hand, the axial force due to the assumed linear distribution must be zero at the net section under pure bending. This means that the assumed linear distribution must be zero at the centre of the current thickness $(h_{\mathrm{t}}+h_{\mathrm{c}})$. The right-hand side of Eq. (2) should thus be integrated from $-(h_{\mathrm{t}}+h_{\mathrm{c}})/2$ to $(h_{\mathrm{t}}+h_{\mathrm{c}})/2$.

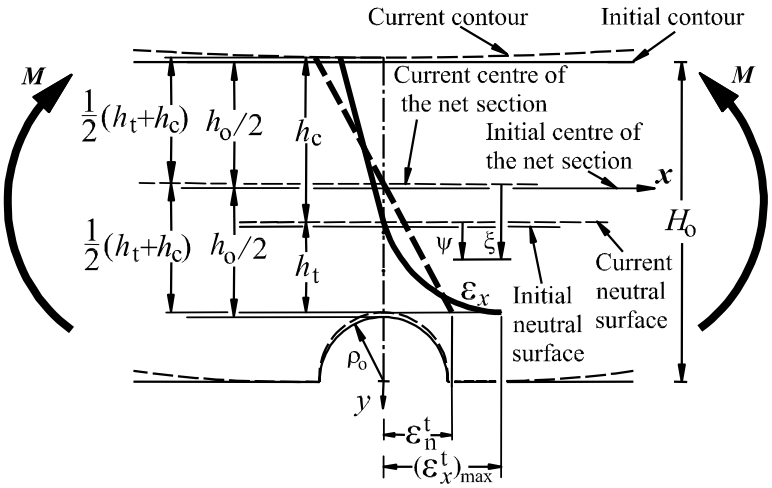

Fig. 1. Initial and current longitudinal sections of a notched rectangular specimen with a single-edge notch.

Eq. (2) presents the following new nominal strain:

$$\varepsilon_n^{new} = \varepsilon_n^t = \frac{6}{(h_t + h_c)^2} \int_{-h_c}^{h_t} \varepsilon_x \psi \, d\psi \tag{3}$$

For plane-strain elastic deformation $\sigma_z = v(\sigma_x + \sigma_y)$, and hence Eq. (3) is transformed into

$$\begin{aligned} \varepsilon_n^{new} &= \phi \left[(1 - v^2) \int_{-h_c}^{h_t} \sigma_x \psi \, d\psi - (v + v^2) \int_{-h_c}^{h_t} \sigma_y \psi \, d\psi \right] \\ &= \phi \left[(1 - v^2) M - (v + v^2) \int_{-h_c}^{h_t} \sigma_y \psi \, d\psi \right] \end{aligned} \tag{4}$$

where $\phi = 6/E(h_t + h_c)^2$.

The conventional SNCF has been defined as

$$K_\varepsilon^{con} = \frac{(\varepsilon_x^t)_{max}}{\varepsilon_n^{con}}$$

where ε_n^{con} is the conventional nominal strain, given by the maximum tensile longitudinal strain at the outside surface of a plane-strain unnotched rectangular bar with the cross-section identical with the net section. This means that ε_n^{con} has been defined under the biaxial stress state, because $\sigma_y = 0$ in unnotched bars. It should be noted that this biaxial stress state is completely unrelated to the stress state at the net section at any deformation level.

For plane-strain elastic deformation, ε_n^{con} is given by

$$\varepsilon_n^{con} = \phi(1 - v^2) M \tag{5}$$

Eqs. (4) and (5) give the following equation:

$$\varepsilon_n^{new} = \varepsilon_n^{con} - \phi(v + v^2) \int_{-h_c}^{h_t} \sigma_y \psi \, d\psi \tag{6}$$

Eqs. (4) and (6) indicate that the new nominal strain in elastic deformation is defined under the triaxial stress state at the net section. In plastically deformed regions the plastic component of the longitudinal

strain is given under the triaxial stress state, as indicated by the theory of plasticity. That is, the magnitude and the distribution of the longitudinal strain ε_x are affected by the magnitudes and the distributions of the three stress components on the net section, namely σ_x, σ_y and σ_z. The theory of plasticity indicates that the plastic component of ε_x is related to the equivalent stress σ_{eq}. The equivalent stress σ_{eq} is a function of the stress differences $(\sigma_x - \sigma_y)^2$, $(\sigma_y - \sigma_z)^2$ and $(\sigma_z - \sigma_x)^2$ (Johnson and Meller, 1983). Accordingly, the new nominal strain, given in Eq. (3), is defined under the triaxial stress state at the net section at any deformation level. This means that the new nominal strain is more logical and more reasonable than the conventional one for the calculations of the SNCF.

3. Specimen geometries

The notched rectangular bars employed have a single-edge U- or circular arc notch on the surface. The thickness of the net section h_0 was varied to examine the effect of the notch depth, whereas the gross thickness H_0 of 16.7 mm was held constant.

The net-to-gross thickness ratio h_0/H_0 is varied from 0.2 to 0.98 to evaluate the effect of notch depth on the new SNCF. Three notch depths of $h_0/H_0 = 0.2$, 0.6 and 0.95 have been selected to discuss the effect of notch depth on the elastic–plastic SNCF. These notch depths given by $h_0/H_0 = 0.2$, 0.6 and 0.95 are referred to as the extremely deep notch, the deep notch and the shallow notch, respectively. Three notch radii ρ_0 of 0.5, 1 and 2 mm are employed to vary the notch sharpness. The width b_0 and half length of the notched specimens are 1 mm and 115 mm, respectively.

4. FEM calculations

A finite element mesh of one half of a notched specimen is shown in Fig. 2. An eight-node element was chosen to model the specimens. The number of nodes and elements are 6133 and 1980, respectively, and the degrees of freedom are 12266.

The FEM calculations were carried out under the plane-strain condition, using the software MARC K6.2 on an APOLLO workstation (MARC User Manual, 1994). The nodal displacement is zero in the x -direction at the net section, and zero in the y -direction at the support.

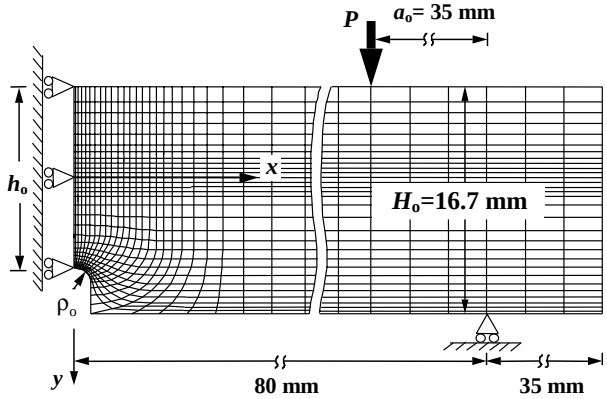

Fig. 2. Finite element mesh and four-point bending.

Four-point bending was employed to provide pure bending, as shown in Fig. 2. The transverse load P was applied at the initial distance a_0 of 35 mm from the support. The initial half length subjected to pure bending is 45 mm, which is a sufficient length to obtain the pure nature of notch effect at the net section. The increment of P is 1 N/mm.

The FEM calculations on the unnotched bar were also performed to obtain the nominal strain for the conventional SNCF. The same conditions as those imposed on the notched bars were employed. The unnotched bar has the cross-section identical with the net section. The half length is 50 mm. The transverse load was applied at $a_0 = 20$ mm from the support. The number of nodes and elements are 4473 and 1440 respectively.

5. Stress–strain relationships

An austenitic stainless steel and an Ni–Cr–Mo steel were used to provide marked differences both in the flow stress and in the rate of strain hardening. The true stress σ-plastic strain ε_p relations were obtained from unnotch tension tests. The results were divided into a few plastic strain ranges to fit the following fifth-degree polynomial accurately:

$$\sigma = C_0 + C_1\varepsilon_p + C_2\varepsilon_p^2 + C_3\varepsilon_p^3 + C_4\varepsilon_p^4 + C_5\varepsilon_p^5$$

The values of the polynomial coefficients and the plastic strain ranges are listed in Table 1, together with Young's modulus E, Poisson's ratio v and tensile yield stress σ_Y. Fig. 3 shows the tensile true stress-plastic strain curves obtained from the polynomials. These curves were also used as the compressive true stress-plastic strain curves. An incremental algorithm follows plastic action as it develops and so accounts for plasticity's path-dependent nature. Each step of the sequence is based on material properties appropriate to that step.

6. Results and discussion

6.1. Effect of the notch depth on elastic K_ε^{new} and K_ε^{con}

Fig. 4 shows the effect of the notch depth on the elastic new and conventional SNCFs. The elastic value of the new SNCF is greater than that of the conventional SNCF. This is independent of notch depth and notch radius. The conventional nominal strain (Eq. (5)) has been defined under biaxial state of stress, while the new nominal strain (Eq. (3)) is defined under triaxial stress state at the net section. The nominal strain under biaxial stress state is larger than that under triaxial stress state. This gives the conventional SNCF an elastic value less than that of the elastic value of the new SNCF. Moreover, the new SNCF is more reliable

Table 1
Elastic constants, tensile yield stresses and polynomial coefficients

Material E (GPa), v, σ_Y (MPa)	Plastic strain range	C_0	C_1	C_2	C_3	C_4	C_5
Austenitic stainless steel	$\varepsilon_p \leqslant 0.2$	2.459×10^2	4.389×10^3	-3.265×10^4	2.402×10^5	-8.899×10^5	1.258×10^6
206.0, 0.30, 245.9	$0.2 < \varepsilon_p \leqslant 0.5$	3.789×10^2	1.535×10^3	1.173×10^3	-1.874×10^3	0.0	0.0
Ni–Cr–Mo steel	$\varepsilon_p \leqslant 0.1$	5.250×10^2	7.644×10^3	-7.377×10^4	2.596×10^5	0.0	0.0
206.0, 0.30, 525.0	$0.1 < \varepsilon_p$	7.426×10^2	6.945×10^2	-8.143×10	0.0	0.0	0.0

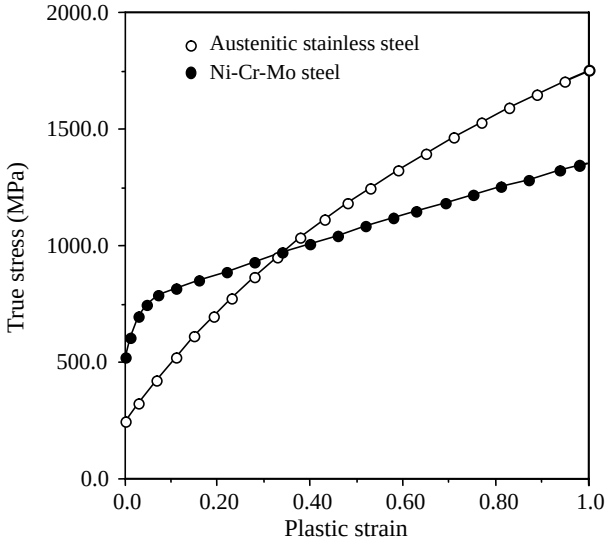

Fig. 3. True stress–plastic strain curves used in the FEM calculations.

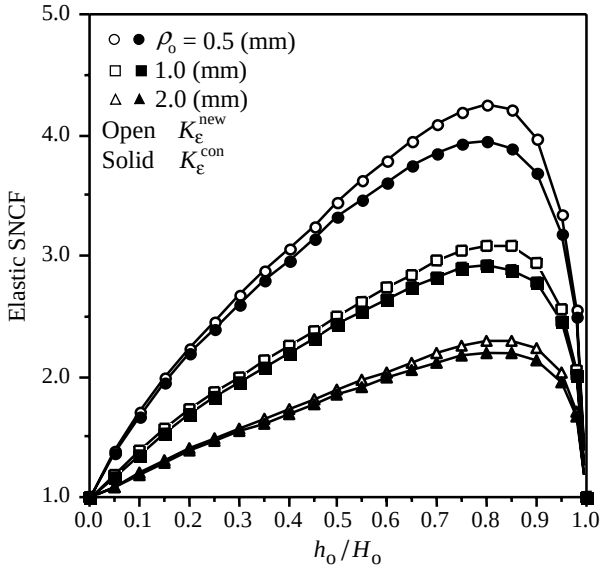

Fig. 4. New and conventional SNCFs in elastic deformation.

than the conventional one; because it expresses the real stress state at the net section, which is triaxial stress state.

The elastic new SNCF increases with increasing net-to-gross thickness ratio h_0/H_0 and reaches its maximum at $h_0/H_0 = 0.8$. By further increasing h_0/H_0, the elastic new SNCF decreases with h_0/H_0. It rapidly decreases especially in the range $h_0/H_0 > 0.85$. The elastic new and conventional SNCFs are approximately equal for shallow notch. This becomes prominent with increasing notch radius. It should be noted that the elastic new SNCF of the shallow notch ($h_0/H_0 = 0.95$) is less that that of the deep notch ($h_0/H_0 = 0.6$).

6.2. Shift of neutral surface

Eq. (3) indicates that the new nominal strain depends strongly on the values of h_c and h_t. Fig. 5 shows the variations in h_c/h_t with bending moment per unit width M ($=Pa$), together with those in the current thickness at the net section ($h_t + h_c$). For symmetrical deep notches the initial value of h_c/h_t is 1.0 irrespective of notch radius (Majima and Ishizaka, 2003), whereas it depends on notch radius for a single-edge notch, ranging from 2.09 to 1.73. The value of h_c/h_t slightly decreases even in elastic deformation. This decrease is less in a single-edge notch than in symmetrical deep notches as given by Majima and Ishizaka (2003). That is, Majima and Ishizaka (2003) have proved that the value of h_c/h_t rapidly decreases from the initial value for the symmetrical deep notches. The rate of decrease in h_c/h_t increases as plastic deformation develops from the notch root and reaches the minimum value around general yielding for $\rho_0 = 0.5$ and 1 mm, and before general yielding for $\rho_0 = 2$ mm. This means that the neutral surface shifts towards the unnotched surface, subjected to compressive ε_x. On further deformation, h_c/h_t shows a rapid increase; that is, the neutral surface shifts towards the notch root. The maximum and minimum values of h_c/h_t are approximately 2.09 for $\rho_0 = 0.5$ mm and 1.48 for $\rho_0 = 2$ mm, respectively. The distances from the notch root to the neutral surface are therefore 64.7% and 80.6% of the current half thickness $(h_t + h_c)/2$, respectively.

Notch radius strongly affects the value of h_c/h_t from elastic deformation up to general yielding. The value of h_c/h_t increases with decreasing notch radius at any deformation level. However, the difference in value is slight around general yielding. It should be noted that for symmetrical deep notches the value of h_c/h_t is nearly independent of notch radius up to general yielding (Majima and Ishizaka, 2003). The value of $(h_t + h_c)$ maintains the initial value h_0 at any deformation level. These are independent of notch radius and notch depth.

6.3. Variations in the new SNCF K_ε^{new} with bending moment M

Fig. 6 shows the variations in K_ε^{new} with M for the deep and shallow notches. For the extremely deep notch the range of M is small because of the small value of h_0. It is thus difficult to show the variation in K_ε^{new} in the same figure. General yielding is not confirmed for the shallow notch in the load range used.

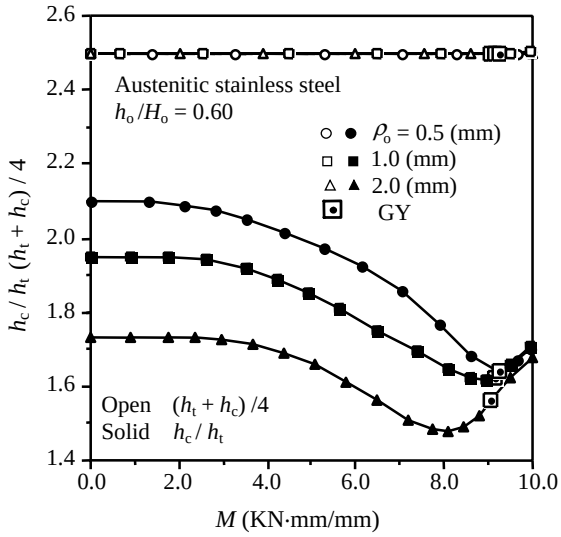

Fig. 5. Variations in h_c/h_t and $h_t + h_c$ with bending moment.

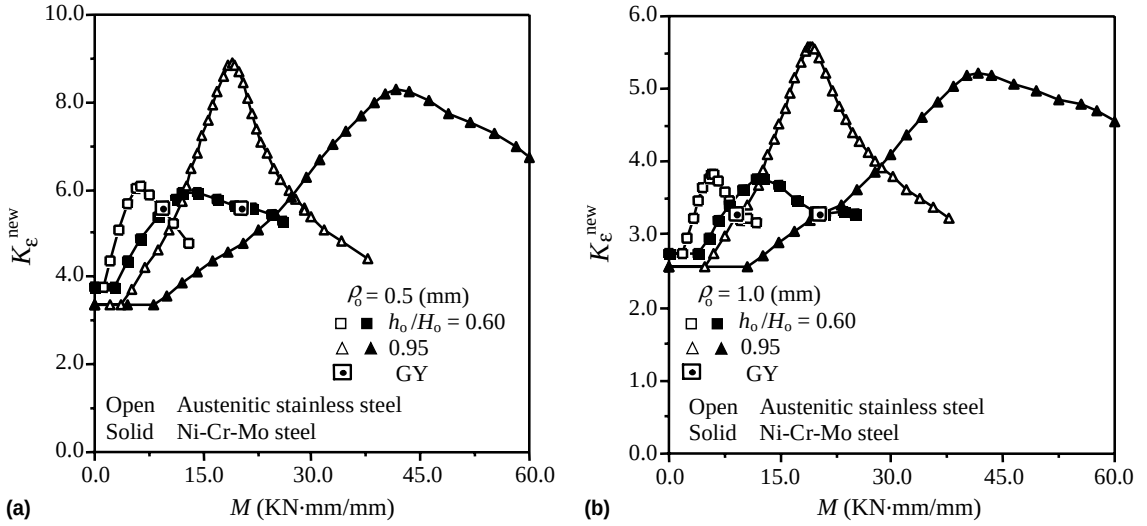

Fig. 6. Variations in K_ε^{new} with bending moment for the deep and shallow notches: (a) $\rho_0 = 0.5$ mm, (b) $\rho_0 = 1.0$ mm.

The stress–strain curve has a strong effect on the variation in K_ε^{new} with M. However, the manner of the increase and decrease in K_ε^{new} is similar irrespective of the stress- strain curve. The new SNCF is constant during elastic deformation. It rapidly increases from its elastic value to the maximum as plastic deformation develops from the notch root.

The bending moment at yielding at the notch root M_Y, at which K_ε^{new} starts to increase, increases with increasing h_0/H_0. This is because the magnitude of M_Y is basically proportional to $(h_0)^3$. The magnitude of M_Y is also affected by the distribution of the longitudinal stress on the net section. This distribution is closely related to notch radius, which dominates the elastic SSCF; this elastic SSCF means the elastic conventional SSCF, which has been defined under the triaxial stress state at the net section (Majima, 1999). The difference in the elastic SSCF, given in Table 2, between $h_0/H_0 = 0.6$ and 0.95 is small compared with the difference in $(h_0)^3$. This provides the increase in M_Y with an increase in h_0/H_0. The value of M_Y is also proportional to the tensile yield stress σ_Y.

On further deformation, K_ε^{new} decreases from its maximum. The maximum K_ε^{new} is much greater than the elastic K_ε^{new} for the shallow notch. Moreover, this maximum K_ε^{new} of the shallow notch is considerably greater than the maximum K_ε^{new} of the deep notch. On the other hand, the elastic K_ε^{new} of the shallow notch is less than that of the deep notch, as clearly shown in Fig. 4. A shallow single-edge notch therefore has a strong effect on strength and fracture under elastic–plastic deformation even if the elastic K_ε^{new} is low.

The sharp decrease from the maximum K_ε^{new} is due to the sharp increase in the new nominal strain ε_n^{new}. Fig. 7 shows that ε_n^{new} rapidly increases after the maximum K_ε^{new}. This is because the longitudinal strain around the notch root rapidly increases owing to the rapid development of the plastic deformation around

Table 2
Elastic new SNCF and elastic SSCF

ρ_0 (mm)	0.5			1.0			2.0		
h_0/H_0	0.20	0.60	0.95	0.20	0.60	0.95	0.20	0.60	0.95
New SNCF	2.240	3.785	3.353	1.721	2.735	2.560	1.405	2.040	2.024
SSCF	2.189	3.619	3.191	1.686	2.645	2.453	1.381	1.988	1.955

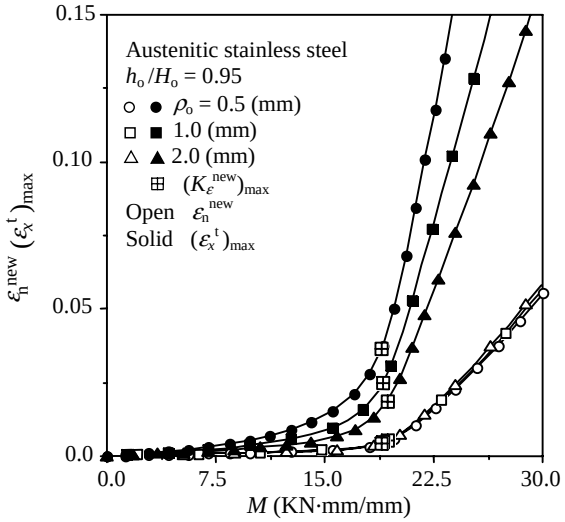

Fig. 7. Variations in ε_n^{new} and $(\varepsilon_x^t)_{max}$ with bending moment.

the notch root. Fig. 8 shows the distributions of the tensile longitudinal strain in the range $0 \leqslant \psi/h_t \leqslant 1.0$ for the shallow notch. The distribution is linear and nearly constant in the range $0 \leqslant \psi/h_t \leqslant 0.8$, and is sharply concave in the range $\psi/h_t > 0.8$. The increase in $(\varepsilon_x^t)_{max}$ after the maximum K_ε^{new} is much greater than that before the maximum K_ε^{new}. This indicates the rapid development of the plastic deformation around the notch root. This causes a high rate of increase in ε_n^{new}. As a result, K_ε^{new} sharply decreases with M.

The rapid increase in K_ε^{new} from its elastic value to the maximum becomes greater with decreasing notch radius for the shallow notch. This is because the increase in $(\varepsilon_x^t)_{max}$, as shown in Fig. 7, increases with decreasing notch radius, while ε_n^{new} is almost independent of notch radius. This independence is due to

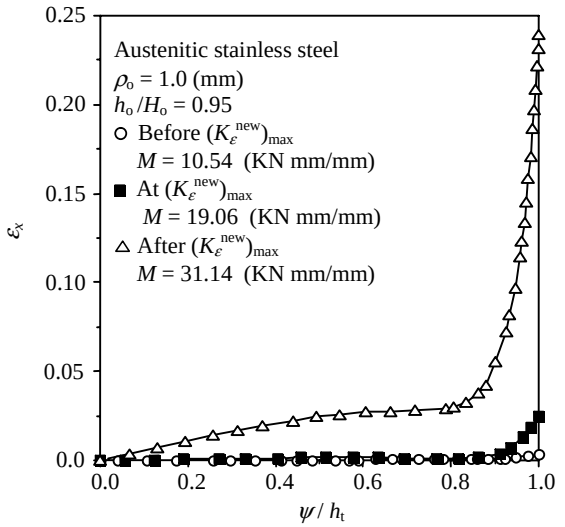

Fig. 8. Effect of deformation on the distributions of ε_x in the range $0 \leqslant \psi/h_t \leqslant 1$.

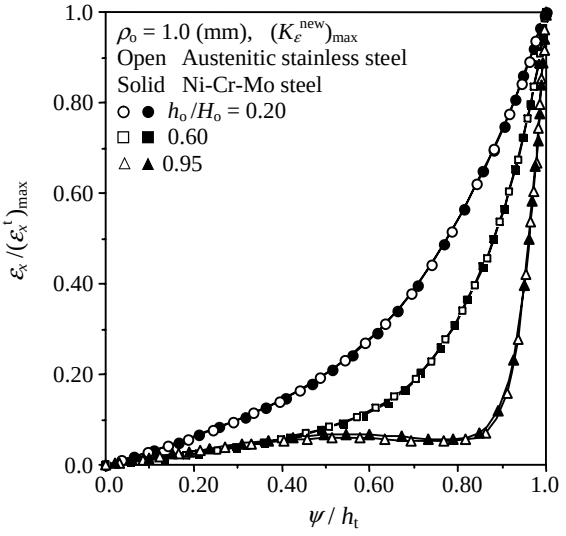

Fig. 9. Effect of notch depth on the distributions of $\varepsilon_x/(\varepsilon_x^t)_{max}$ in the range $0 \leqslant \psi/h_t \leqslant 1$.

the concentration of the plastic deformation in a small area around the notch root. This occurs when the notch radius of a shallow single-edge notch is sufficiently small compared with the initial thickness h_0.

Fig. 9 shows the distributions of the normalized longitudinal strain $\varepsilon_x/(\varepsilon_x^t)_{max}$ at the maximum K_ε^{new} in the range $0 \leqslant \psi/h_t \leqslant 1.0$; the distribution on the net section is schematically shown in Fig. 1. The distribution in the range $\psi/h_t > 0.8$ is sharply concave for the shallow notch. On the other hand, the distribution in the range $0 \leqslant \psi/h_t \leqslant 1.0$ is mildly concave for the deep notch, and is more mildly concave for the extremely deep notch. Fig. 9 also indicates that the distributions of $\varepsilon_x/(\varepsilon_x^t)_{max}$ on the net section are independent of the stress–strain curve. This suggests that the deformation level at the maximum K_ε^{new} is the same even if the value of M at the maximum K_ε^{new} is different because of the difference in the stress–strain curve.

6.4. The significance of the new SNCF

Comparisons between the new and conventional SNCFs are made in Fig. 10. The conventional SNCF K_ε^{con} increases from its elastic value to the maximum, which is greater than the maximum K_ε^{new}. On further deformation, it rapidly decreases to approximately unity or less than unity. This rapid decrease is caused by the rapid increase in the conventional nominal strain ε_n^{con}. This is because ε_n^{con} is obtained under the biaxial stress state of the plane-strain unnotched bar. That is, the longitudinal strain under the biaxial stress state becomes much greater than that under the triaxial stress state. For this reason K_ε^{con} becomes much less than K_ε^{new} and decreases to the values less than unity.

Fig. 11 shows the distributions of transverse stress σ_y on the net section. The value of σ_y is equal to zero at the notch root and at the unnotched surface opposite to the notch root, while it is different from zero through the net section. This is independent of the notch depth and of the notch radius. This means that

$$\int_{-h_c}^{h_t} \sigma_y \psi \, d\psi \neq 0$$

at any deformation level, and hence the effect of σ_y can not be neglected. Therefore, the conventional nominal strain ε_n^{con}, neglecting the effect of σ_y, is unreasonable for the calculation of the SNCF.

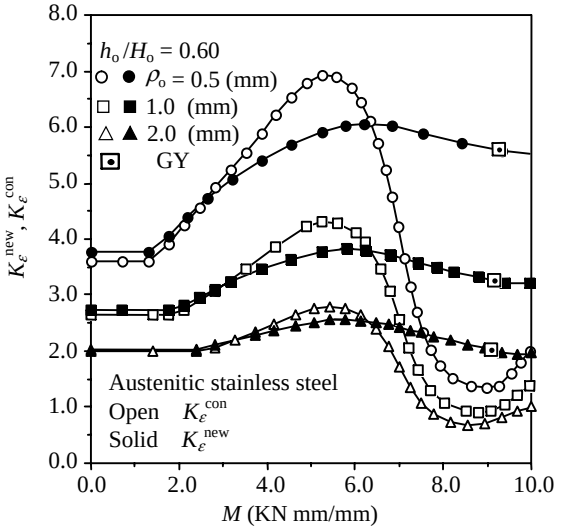

Fig. 10. Comparisons of K_ε^{new} with K_ε^{con}.

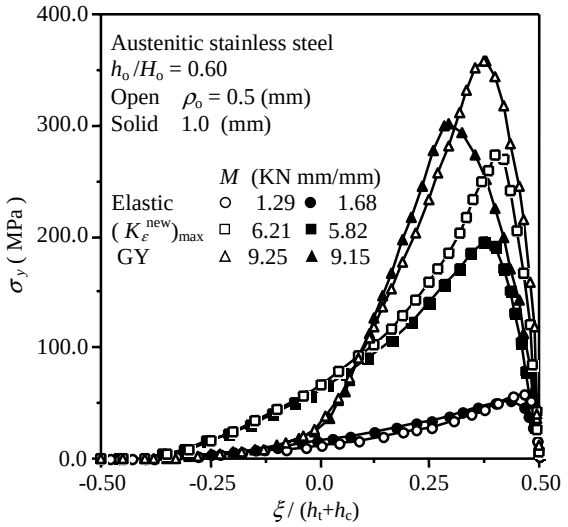

Fig. 11. Distributions of σ_y on the net section in the range $-0.5 \leqslant \xi/(h_t + h_c) \leqslant 0.5$.

Moreover, the non-linear distributions of $\varepsilon_x/(\varepsilon_x^t)_{max}$, shown in Fig. 9, require that the SNCF should be greater than unity irrespective of deformation level. Fig. 10 shows that $K_\varepsilon^{new} > 1.0$ even at the general yielding, whereas $K_\varepsilon^{con} \leqslant 1.0$. The definition of K_ε^{con} is thus unreasonable also for a single-edge notch as well as for the symmetrical deep notches (Majima and Ishizaka, 2003). The present results and the results given by Majima and Ishizaka (2003) clearly suggest that K_ε^{new} is more reasonable than the K_ε^{con} of predicting strength and fracture of the notched bars.

For pure bending, the SSCF has been defined as the ratio of the longitudinal stress σ_x at the notch root to the nominal stress $\sigma_n(= 6M/b_0h_0^2)$, (Leven and Frocht, 1952; Kosmatka et al., 1990; Pilkey, 1997). In the

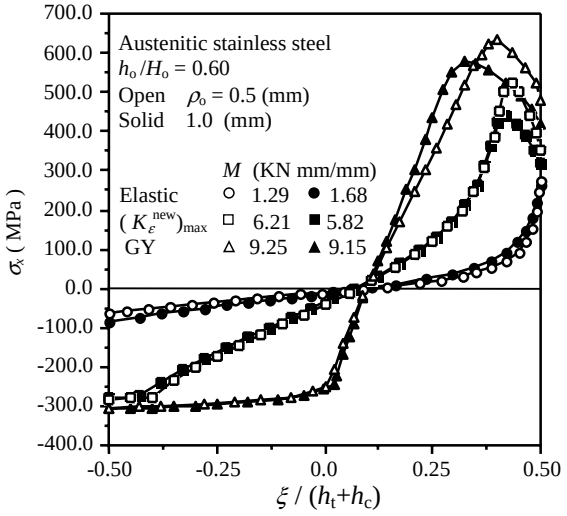

Fig. 12. Distributions of σ_x on the net section in the range $-0.5 \leqslant \xi/(h_t + h_c) \leqslant 0.5$.

elastic deformation, Fig. 12 shows that the longitudinal stress has a concave distribution on the net section, and σ_x at the notch root is equal to the maximum longitudinal stress (Leven and Frocht, 1952; Nishida, 1974; Kato, 1991; Noda et al., 1995; Pilkey, 1997). The concave distribution of σ_x becomes mild or mildly convex as the plastic deformation develops from the notch root. The maximum σ_x lies some way from the notch root inside the plastic zone, as clearly shown in Fig. 12. The σ_n becomes greater than σ_x at the notch root. Thus, the elastic–plastic SSCF rapidly decreases from its elastic value to unity as the plastic develops from the notch root. This means that the stress concentration disappears; and the SSCF no longer appropriate to predict strength and fracture of the notched bars under elastic–plastic deformation. Therefore, the new SNCF is more reasonable of predicting strength and fracture of the notched bars.

6.5. Effect of the stress–strain curve on the new SNCF

The parameter M/M_Y can eliminate the difference in the stress–strain curve from the K_ε^{new} versus M/M_Y relation for the symmetrical deep notches. This is true even if there is a marked difference (Majima and Ishizaka, 2003) shown in Fig. 3. Fig. 13 shows the variations in K_ε^{new} with M/M_Y for the three notch depths. It should be noted that the use of M/M_Y makes it possible to draw this variation of the extremely deep notch in the same figure.

The new SNCF increases from its elastic to the maximum and decreases after that. This is independent of notch depth. The increase in K_ε^{new} from the elastic K_ε^{new} to the maximum increases with decreasing notch depth. This increase is remarkable for the shallow notch. This indicates the localization of plastic deformation around the notch root. In contrast, the increase is very small for the extremely deep notch.

The variation in K_ε^{new} is independent of the stress–strain curve for the deep and extremely deep notches. On the other hand, it is slightly dependent up to the maximum K_ε^{new} for the shallow notch. This dependence is remarkable after the maximum K_ε^{new}.

The independence of the variation in K_ε^{new} with M/M_Y from the stress–strain curve is closely related to the distribution of the longitudinal stress σ_x. The distribution of the normalized longitudinal stress σ_x/σ_Y determines the ratio of bending moment to tensile yield stress M/σ_Y, i.e.

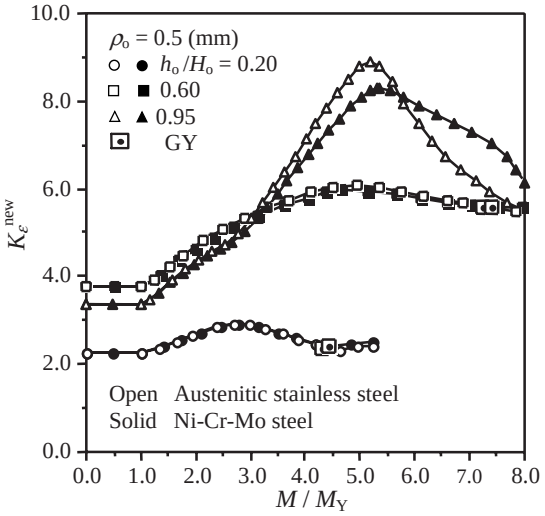

Fig. 13. Variations in K_ε^{new} with M/M_Y for the three notch depths.

$$\int_A \frac{\sigma_x}{\sigma_Y}\psi \, dA = \frac{1}{\sigma_Y}\int_A \sigma_x \psi \, dA = \frac{M}{\sigma_Y} \tag{7}$$

where A is the net area. On the other hand, the theory of elasticity shows that the distributions of σ_x depend only on the notch geometry

$$\sigma_x = (\sigma_x^t)_{max} f(\psi) \tag{8}$$

Moreover, the equivalent stress at the notch root under the plane-strain elastic deformation is given by

$$(\sigma_{eq})_{max} = \sqrt{1 - \nu + \nu^2}(\sigma_x^t)_{max} \tag{9}$$

where $(\sigma_{eq})_{max}$ and $(\sigma_x^t)_{max}$ denote the maximum equivalent stress and the maximum tensile longitudinal stress at the notch root, respectively. The theory of elasticity shows that the magnitude of σ_x on the net section is proportional to M. Consequently $(\sigma_{eq})_{max}$ shows a linear increase with an increase in M. At the onset of yielding at the notch root $(\sigma_{eq})_{max}$ is equal to σ_Y; then Eq. (9) becomes

$$\sigma_Y = \sqrt{1 - \nu + \nu^2}(\sigma_x^t)_{max} \tag{10}$$

This equation can be transformed to

$$(\sigma_x^t)_{max} = \frac{\sigma_Y}{\sqrt{1 - \nu + \nu^2}} \tag{11}$$

Substitution of Eq. (11) into Eq. (8) gives that

$$\sigma_x = \frac{\sigma_Y}{\sqrt{1 - \nu + \nu^2}} f(\psi) \tag{12}$$

This means that M_Y is proportional to σ_Y as indicates by the following relation:

$$\begin{aligned} M &= \int_A \sigma_x \psi \, dA \\ M_Y &= \int_A \frac{\sigma_Y}{\sqrt{1 - \nu + \nu^2}} f(\psi)\psi \, dA = \frac{\sigma_Y}{\sqrt{1 - \nu + \nu^2}} \int_A f(\psi)\psi \, dA \end{aligned} \tag{13}$$

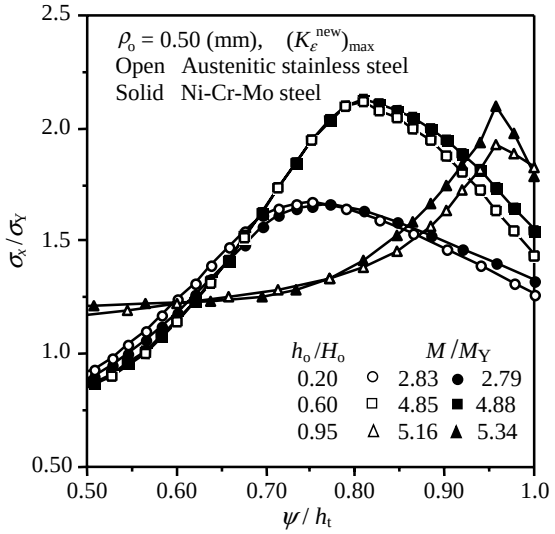

Fig. 14. Effect of the stress–strain curve on the distributions of σ_x/σ_Y.

then, M_Y is proportional to σ_Y because

$$M_Y = \alpha\sigma_Y \tag{14}$$

where $\alpha = \text{constant} = \frac{1}{\sqrt{1-\nu+\nu^2}} \int_A f(\psi)\psi \, dA$.

The parameter M/M_Y is thus directly related to the distribution of σ_x/σ_Y as shown in the following equation, which is derived from Eqs. (7) and (14)

$$\frac{M}{\sigma_Y} = \frac{M}{M_Y/\alpha} = \alpha\frac{M}{M_Y}$$

Fig. 14 shows the distributions of σ_x/σ_Y on the net section for the three notch depths. There is little difference in the distribution of σ_x/σ_Y between two materials for the deep and extremely deep notches. On the other hand, the clear difference is recognized in the range $0.8 \leqslant \psi/h_t \leqslant 1.0$ for the shallow notch. This clear difference brings about the dependence of K_ε^{new} on the stress–strain curve.

7. Conclusions

The effect of notch depth on the new SNCF K_ε^{new} has been studied for plane-strain rectangular bars with a single-edge U- or circular arc notch under pure bending. This new SNCF has been defined under the triaxial stress state at the net section. This has enabled the new SNCF to provide reasonable values for the non-linear distributions of the longitudinal strain. The elastic SNCF versus net-to-gross thickness ratio h_0/H_0 curve is convex with a maximum value at approximately $h_0/H_0 = 0.8$. Beyond this value of h_0/H_0 the elastic SNCF rapidly decreases towards the unity at $h_0/H_0 = 1.0$. The new SNCF increases from its elastic value to the maximum and decreases after that. This is independent of notch depth. The maximum K_ε^{new} of the shallow notch ($h_0/H_0 = 0.95$) is considerably greater than that of the deep notch ($h_0/H_0 = 0.60$), while the elastic K_ε^{new} of the shallow notch is less than that of the deep notch. The plastic deformation around the notch root has a strong effect on the rapid increase in K_ε^{new} for the shallow notch. This is because plastic deformation is restricted in the narrow area around the notch root. The rate of decrease from the maximum

$K_{\varepsilon}^{\text{new}}$ increases with decreasing notch depth. The variation in $K_{\varepsilon}^{\text{new}}$ with M/M_{Y} is dependent on the stress–strain curve for the shallow notch. This dependence is slight up to the maximum $K_{\varepsilon}^{\text{new}}$. On the other hand, the variation in $K_{\varepsilon}^{\text{new}}$ with M/M_{Y} is independent of the stress–strain curve for the deep and extremely deep notches.

References

Johnson, W., Meller, P.B., 1983. Engineering Plasticity. Ellis Horwood Limited, England.

Kato, A., 1991. Design equation for stress concentration factors of notched strips and grooved shafts. J. Strain Anal. 26, 21–28.

Kosmatka, J.B., Fries, R.H., Reinholtz, C.F., 1990. Tension and bending stress concentration factors in '*U*', '*V*', and opposed '*U*' – '*V*' notches. J. Strain Anal. 25, 233–240.

Leven, M.M., Frocht, M.M., 1952. Stress-concentration factors for single notch in flat bar in pure and central bending. J. Appl. Mech. 74, 560–561.

Majima, T., 1999. Strain-concentration factor of circumferentially notched cylindrical bars under static tension. J. Strain Anal. 34, 347–360.

Majima, T., Ishizaka, T., 2003. Strain-concentration factor of plane-strain notched rectangular bars under pure bending. J. Strain Anal. 38, 483–491.

MARC User Manual, 1994. Vol. C (Program Input). MARC Analysis Research Corporation, C2-24, C3-228 and C5-33.

Neuber, H., 1961. Theory of stress concentration factor for shear-strained prismatical bodies with arbitrary nonlinear stress–strain law. J. Appl. Mech. 28, 544–550.

Nishida, K., 1974. Stress Concentration. Morikita Shuppan, Tokyo (in Japanese).

Noda, N.-A., Sera, M., Takase, Y., 1995. Stress concentration factors for round and flat test specimens with notches. Int. J. Fatigue 17, 163–178.

Pilkey, W.D., 1997. Peterson's Stress Concentration Factors. John Wiley & Sons, New York.